Journal of Power Sources 195 (2010) 4255–4265

Contents lists available at ScienceDirect

Journal of Power Sources

journal homepage: www.elsevier.com/locate/jpowsour

Mechanism study of enhanced electrochemical performance of ZrO_2-coated $LiCoO_2$ in high voltage region

B.J. Hwang[a,b,*], C.Y. Chen[a], M.Y. Cheng[a], R. Santhanam[a], K. Ragavendran[a]

[a] Nanoelectrochemistry Laboratory, Department of Chemical Engineering, National Taiwan University of Science and Technology, 43 Keelung Road, Sec. 4, Taipei 106, Taiwan, ROC
[b] National Synchrotron Radiation Research Center, Hsinchu 300, Taiwan, ROC

ARTICLE INFO

Article history:
Received 25 August 2009
Received in revised form 8 January 2010
Accepted 21 January 2010
Available online 25 January 2010

Keywords:
Lithium cobalt oxide
Zirconia coating
Stability
High voltage
Lithium ion battery
Cathode

ABSTRACT

In this study, the mechanism of enhanced performance of ZrO_2-coated $LiCoO_2$ especially at high potential range is systematically investigated. Firstly, when overcharging to 4.5 V (higher than 4.2 V, the normal cutoff charging potential), phase transformation from H1 to H2 takes place with less volume expansion for ZrO_2-coated $LiCoO_2$ (1.2% and 2.2% for as-received one). EIS analysis indicates the growth of interfacial impedance during charging/discharging can be effectively suppressed with ZrO_2 coating on the $LiCoO_2$ surface. It is demonstrated as well that cation mixing of the cycled $LiCoO_2$ caused by re-intercalation of dissolved Co^{2+} is inhibited with the ZrO_2 coating on the $LiCoO_2$. Therefore the ZrO_2-coated $LiCoO_2$ shows great enhancement in the electrochemical properties with 85% capacity retention after 30 cycles from 3 to 4.5 V at a rate of 0.5*C*. Nevertheless, under the same evaluation process, the as-received $LiCoO_2$ possesses only 21% capacity retention, which is resulted from the formation of polymeric layers by the electrolyte decomposition on its surface, the higher volumetric changes during charging/discharging and possible cation mixing by re-intercalation of the dissolved Co^{2+}.

1. Introduction

Since the introduction of $Li_xC_6/Li_{1-x}CoO_2$ rechargeable battery into the market by Sony nearly 20 years ago, $LiCoO_2$ is the most widely used cathode material in commercial lithium ion batteries due to its good balance between high energy density and cycling performance. Among the hexagonal α-$NaFeO_2$-type oxide materials such as $LiNiO_2$ and $LiMnO_2$, $LiCoO_2$ is the most stable cathode material [1–3]. However, the charging limit is critical for a lithium ion battery when $LiCoO_2$ is used as the cathode material. The practical capacity of $Li_{1-x}CoO_2$ remains 140 mAh g^{-1} for $x = 0.5$ when it is charged up to 4.2 V, which is 50% of the theoretical capacity of 274 mAh g^{-1}. The limitation is owing to its structural instability for $x > 0.5$, where collapse of the crystalline structure takes place rapidly. Another issue is the surface instability of $LiCoO_2$ due to reactions with the electrolyte [4,5]. To solve this problem, many studies have been carried out on the improvement of $LiCoO_2$ cathode materials [6–15].

Cho et al. [8,9] have first reported that a thin coating of high-fracture-toughness metal oxides on $LiCoO_2$ can suppress the lattice constant changes and hence suppress the phase transitions and improve capacity retention during electrochemical cycling to 4.4 V. Based on this result, Cho et al. called ZrO_2-coated $LiCoO_2$ a "zero-strain" cathode for lithium ion batteries. The suppression of phase transitions has been further supported by using slow-scan cyclic voltammetry data obtained at an upper voltage limit of 4.4 V [16]. However, the mechanism of capacity fading of oxide-coated $LiCoO_2$ during high voltage cycling was questioned by Chen and Dahn [10]. They showed that ZrO_2 coating on the cathode material does not affect the lattice constant changes, in contrast to the results reported by Cho et al. [8,9]. They believed that the coating might inhibit side reactions involving oxygen loss by reducing the contact area between $LiCoO_2$ and the electrolyte. Chen and Dahn have also reported that the capacity retention of $LiCoO_2$ was improved by a simple heat treatment which causes the elimination of surface moisture and chemical species [17]. Recently, Appapillai et al. have shown that improved performance of $AlPO_4$-coated $LiCoO_2$ to bare $LiCoO_2$ is due to a difference in the surface microstructure rather than structural instability [18]. Liu et al. studied the effect of Al_2O_3 coating on the cycling performance during high voltage cycling and proposed the mechanism from the point of view of structural changes [19]. According to Kim et al. the improved capacity retention is due to the suppression of cobalt dissolution

* Corresponding author at: Nanoelectrochemistry Laboratory, Department of Chemical Engineering, National Taiwan University of Science and Technology, 43 Keelung Road, Sec. 4, Taipei 106, Taiwan, ROC. Tel.: +886 2 27376624; fax: +886 2 27376644.
E-mail address: bjh@mail.ntust.edu.tw (B.J. Hwang).

0378-7753/$ – see front matter © 2010 Elsevier B.V. All rights reserved.
doi:10.1016/j.jpowsour.2010.01.040

from the $LiCoO_2$ cathodes with various metal oxide coatings [20]. However, the mechanism underlying the improved performance in metal oxide-coated cathode materials is still under controversy, and requires further investigations.

In our previous works, the influence of protective coatings on the electrochemical performance of $LiMn_2O_4$ is studied [21]. Observation on the cycle life improvement in ZrO_2-coated spherical $LiNi_{1/3}Co_{1/3}Mn_{1/3}$ cathode material was reported [22]. The improvement is attributed to be free from HF attack by ZrO_2-coating protection, which would not effect the Li^+ insertion/de-insertion reactions. Investigation on ZrO_2-coated $LiMn_{0.5}Ni_{0.5}O_2$ cathode indicates the improved performance is owing to a combination of two factors, viz. inhibition of electrolyte decomposition on the surface and to the stabilization of the layered structure [23]. In this study, the aid of in situ XRD has made further advancements in our understanding on the role played by ZrO_2 protective coatings, especially in the high voltage region.

2. Experimental section

Commercially available $LiCoO_2$ material obtained from CERAC was used as received. The heat-treated $LiCoO_2$ materials were prepared by heating the as-received $LiCoO_2$ at 900 °C with a heating rate of 2 °C min^{-1}. The ZrO_2-coated $LiCoO_2$ materials were prepared by dispersing calculating amount of the commercial as-received $LiCoO_2$ and $Zr(OC_3H_7)_4$ in 1-propanol such that the final product with 0.5 wt% ZrO_2-coating layer was obtained. The entire process was carried out under continuous stirring at 80 °C until fully removal of the solvent. The resulting precursor was heated at 400 °C for 10 h to obtain the ZrO_2-coated $LiCoO_2$.

X-ray diffraction measurements were carried out with a Rigaku D/Max-RC X-ray diffractometer using Cu-Kα as the radiation source. Scanning electron microscopy and transmission electron microscopy characterizations were carried out, respectively, with a JEOL JSM-6500F and JEOL JEM-1010 equipments. Electrochemical impedance spectroscopy measurements were performed using an impedance analyzer (Solartron 1260 + 1286) over the frequency range from 10^6 to 10^{-3} Hz with the amplitude of 10 mV. Differential scanning calorimetry experiments were carried out with PerkinElmer Pyris 1. In situ X-ray diffraction (XRD) measurements were carried out with synchrotron radiation source at beam line 01C2 in the National Synchrotron Radiation Research Center (NSRRC), Hsinchu, Taiwan. The beam line was operated at the energy of 25 keV (wavelength (ë) = 0.5166 Å). The optical design for the monochromatic beam is described as follows: the first mirror focusing at the beam vertically and asymmetrically cut and horizontally bendable a perfect single crystal as the diffraction object monochromatically focused the beam. A single crystal of Si(1 1 1) with about 10% asymmetric cutting was used to deliver a monochromatic beam size 1 mm in diameter with a single spot at the sample, which is about 24 and 6 m away from the source and monochromatic, respectively. Flat imaging plane was used as a 2D detector. The XRD pattern was read out by aMAC IPR420 off-line imaging plate scanner.

The as-received, heat-treated or ZrO_2-coated $LiCoO_2$ materials were mixed with carbon black, KS6 graphite and polyvinylidene fluoride binder in a ratio of 85:3.5:1.5:10 (w/w), respectively, in N-methylpyrrolidinone to fabricate the positive electrodes. The resulting slurry was coated on an aluminum current collector. The entire assembly was dried at 120 °C under vacuum overnight. Lithium metal (FMC Corporation) was used as anode and a polypropylene separator was used to separate the anode and the cathode. The electrolyte solutions were 1.0 M $LiPF_6$ in ethylene carbonate (EC)–diethyl carbonate (DEC) (1:1 in volume). Studies on the additives in electrolyte to Li^+ insertion/de-insertion were performed with 1.0 M $LiPF_6$ in EC–DEC with additional 5.5 ppm Co or 0.01 M $NaPF_6$. The fabrication of the cell was done in an argon-filled glove box where both moisture and oxygen content were less than 1 ppm. The cells, then, were charged and discharged in different voltage ranges at room temperature.

3. Results and discussion

The crystal structures of the as-received, heat-treated and ZrO_2-coated $LiCoO_2$ particles were characterized by XRD and are shown in Fig. 1. All the diffraction peaks could be attributed to the typical hexagonal phase with space group of R-3m. The lattice parameters of the ZrO_2-coated $LiCoO_2$ (c = 14.03 Å, a = 2.81 Å) are the same as that of heat-treated (c = 14.01 Å, a = 2.81 Å) and as-received (c = 14.03 Å, a = 2.81 Å) $LiCoO_2$. On the other hand, no peak is contributed from ZrO_2-coating layer. It is suggested that the bulk properties of $LiCoO_2$ did not change with ZrO_2 coating.

The surface morphologies of the as-received, heat-treated and ZrO_2-coated $LiCoO_2$ were investigated by SEM (Fig. 2). It is clear that the surface of both the bare and heat-treated $LiCoO_2$ appears to be fairly smooth with clear outlines. Some small particles seem to adhere on the surface of ZrO_2-coated $LiCoO_2$ and can be considered as the ZrO_2 layer. To gain further insight into the microstructure of the cathode particles, TEM studies were performed. Fig. 3 shows TEM images of as-received (a), heat-treated (b) and ZrO_2-coated $LiCoO_2$ (c) under different magnifications. Similar to SEM image, the appearance of heat-treated $LiCoO_2$ particles is fairly smooth. However, the as-received $LiCoO_2$ shows non-smooth surfaces with small particles. The inconsistency may be due to lower resolution of SEM image. The small particles on the outer surface of the as-received $LiCoO_2$ may be owing to reaction with moisture, as concluded in the literature [17]. The TEM images of ZrO_2-coated $LiCoO_2$ shows a uniform ZrO_2 layer composted of small nanoparticles. It is suggested that reduction in the contact area between $LiCoO_2$ and electrolyte by the formed ZrO_2 layer prevents from the interfacial reaction, especially at high voltage.

In situ XRD was employed to study the effects of ZrO_2 coating on the structural changes of $LiCoO_2$ during charge/discharge cycling and their relationship to the capacity retention. The XRD patterns were collected during charging the electrochemical cell from open circuit potential (OCP) to cutoff potential of 5.5 V. Fig. 4a shows the

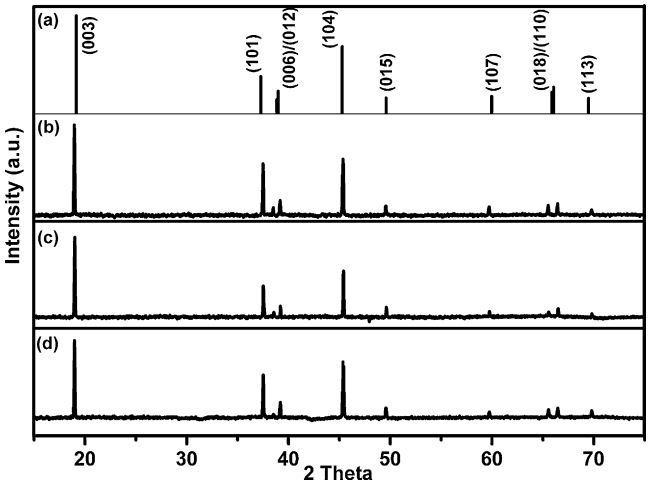

Fig. 1. XRD patterns of (a) JCPDS, (b) as-received, (b) heat-treated and (d) ZrO_2-coated $LiCoO_2$, respectively.

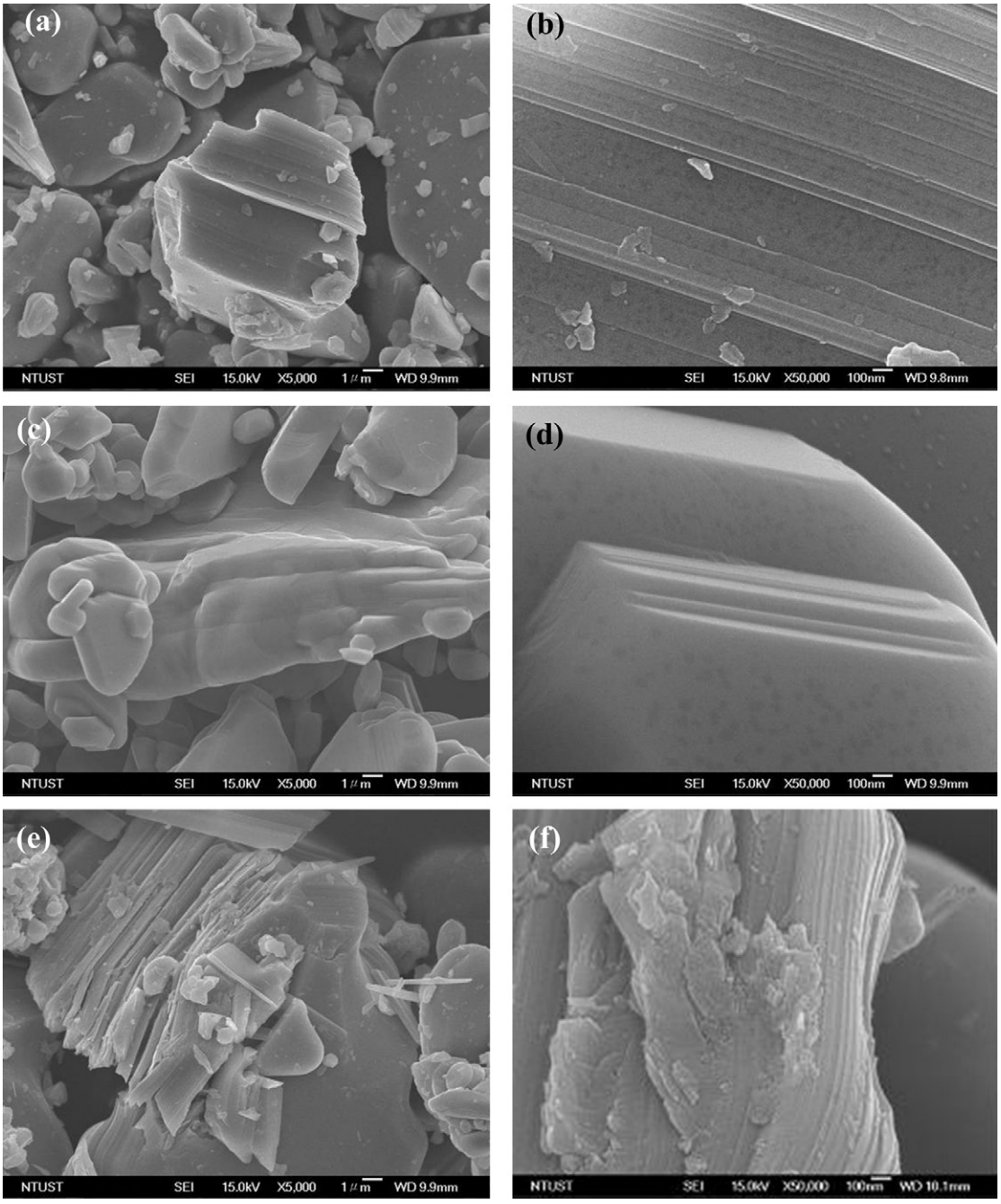

Fig. 2. SEM images of as-received (a and b), heat-treated (c and d) and ZrO_2-coated (e and f) $LiCoO_2$ under low and high magnifications, respectively.

1st charge curve of the as-received $LiCoO_2$-assembled cell up at a rate of 0.1*C*. The wiggles after the capacity of 280 mAh g^{-1} indicate the presence of electrolyte decomposition. The charge states for the acquired XRD patterns are denoted in Fig. 4a and the corresponding patterns are shown in Fig. 4b.It is clear that the as-received $LiCoO_2$ undergoes a series of phase transformations from first hexagonal phase (H1, points 1–7) through second hexagonal one (H2, points 8 and 9) to the final monoclinic one (O1, points 10 and 11), which is consistent with the results reported in the literature [24,25]. Comparing with the ZrO_2-coated $LiCoO_2$ under the same charging conditions as the as-received $LiCoO_2$, similar phase transformation is observed (Fig. 5), The wiggles, observed in the high voltage region for the as-received $LiCoO_2$ cathode, were obviously reduced for ZrO_2-coated $LiCoO_2$ one. This result is believed to be due to suppression of the electrolyte decomposition at high voltage region by the surfaced ZrO_2 coating. Carefully evaluating the change of the crystalline structure of the as-received and the ZrO_2-coated $LiCoO_2$ at each state, the variation of lattice parameters can be obtained (Fig. 6). Basically, it appears that the change of lattice parameters for the as-received sample was similar to that of the ZrO_2-coated one and the change is only observed in *c*-axis direction. The volume expansion, during phase transition from H1 to H2 when charging to 4.5 V, was calculated to be 2.2% and 1.2% for as-received and ZrO_2-coated $LiCoO_2$, respectively (Fig. 6). It is reasonable that the lower volume expansion observed for ZrO_2-coated $LiCoO_2$ should be contributed from the surfaced ZrO_2 coating, which would possibly improve the capacity retention and rate capability when increasing the cutoff voltage to 4.5 V. Further, the inhibition of the H1-to-H2

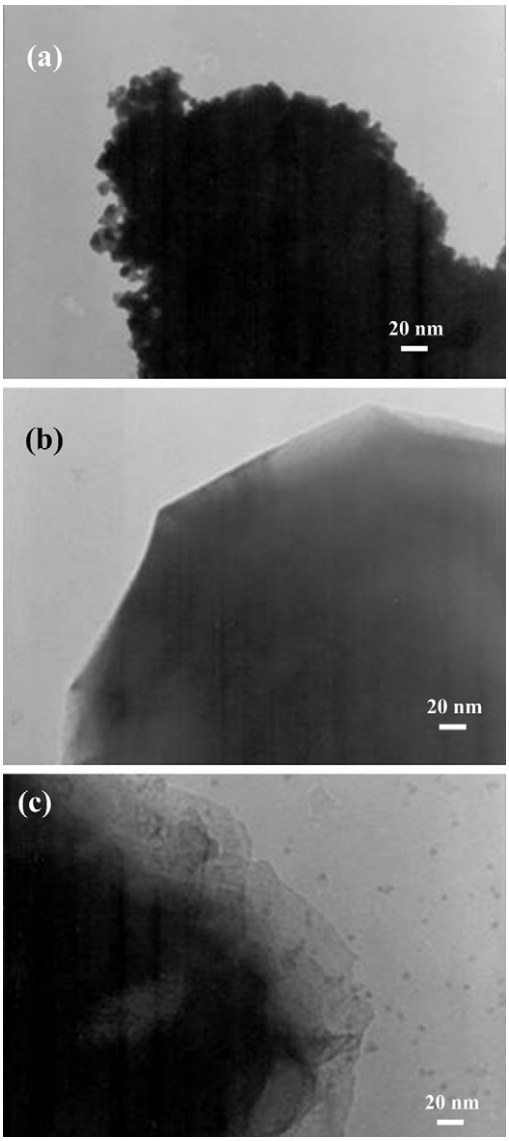

Fig. 3. TEM images of (a) the as-received, (b) heat-treated and (c) ZrO_2-coated $LiCoO_2$.

transition to prolonged charging state is observed, which may be resulted from the ZrO_2 coating as well. Therefore, the observation of lattice expansion in *c*-axis direction of $LiCoO_2$ is again confirmed. However, it takes place after 4.5 V for ZrO_2-coated $LiCoO_2$ in our case, in which the cutoff voltage is 4.4 V for the studies by Cho et al. It may not reach the state of H1-to-H2 phase transition.

Fig. 7 shows the electrochemical impedance spectroscopy (EIS) experiments performed to investigate the resistance distribution in the lithium cell assembled with as-received, heat-treated or ZrO_2-coated $LiCoO_2$ electrodes cycled between 3.0 and 4.5 V at a rate of 0.5*C*. In general, each impedance spectrum consists of three parts. The first semicircle at the high frequency region can be assigned to resistance of the lithium ions migration in the electrolyte between the two electrodes in the cell. The second semicircle at medium-to-low frequency region explains charge transfer resistance at the electrode/electrolyte interface where electrochemical reaction taking place on. The sloping line in the very low frequency region is associated with the lithium ion diffusion in the bulk of the active material. The R_b, R_{sf}, R_b, and R_{ct} values obtained for the cells assembled with as-received, heat-treated and ZrO_2-coated $LiCoO_2$ electrodes are given in Table 1 along with the equivalent circuit used to calculate the resistance values. It was reported that the cell impedance was mainly determined by the charge transfer resistance arising from the cathode material. It was found that R_{ct} of the as-received, heat-treated and ZrO_2-coated $LiCoO_2$ was 188 Ω, 45 Ω and 14 Ω after 1st cycle and 10333 Ω, 809 Ω and 39 Ω after 30th cycle, respectively. Thus, it is obvious that the R_{ct} of the as-received sample increases drastically during cycling while only slightly increase of the impedance for the heat-treated and ZrO_2-coated samples. Further considering the difference between the heat-treated and ZrO_2-coated samples, ZrO_2-coating layer significantly suppressed the growth of the R_{ct} which can be seen in Fig. 7c. This may be explained by the fact that the surface film formations are restrained and the decomposition of electrolyte is suppressed at higher potentials on the surface of the ZrO_2-coated $LiCoO_2$. These EIS results are in good agreement with the changes in the charge and discharge profiles in different voltage ranges as discussed below.

Higher capacity and better cycling performance were achieved for ZrO_2-coated $LiCoO_2$ material compared to that of as-received and heat-treated $LiCoO_2$ materials. However, side reactions like dissolution of cobalt into the electrolyte reported by several authors must be addressed [7,15]. It is pertinent to mention here about a crystal shape algorithm [26] using which manganese dissolution in $Li_xMn_2O_4$ prepared through different methods was studied

Table 1
Electrolyte resistance (R_e), surface film resistance (R_{sf}), bulk resistance (R_b) and charge transfer resistance (R_{ct}) for the as-received, and heat-treated and ZrO_2-coated $LiCoO_2$ electrodes and the corresponding equivalent circuit.

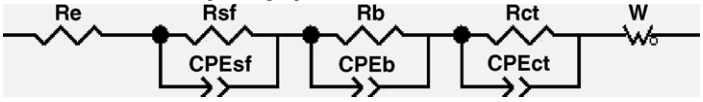

Material	Cycle no.	R_e (Ω)	R_{sf} (Ω)	R_b (Ω)	R_{ct} (Ω)
As-received $LiCoO_2$	1	7.9	27.9	711.1	188.1
	10	7.0	16.4	1685.0	2,726.0
	20	7.2	35.2	1914.0	10,092.0
	30	14.5	12.5	4632.0	10,333.0
Heat-treated $LiCoO_2$	1	4.9	4.4	73.1	44.9
	10	5.3	4.9	64.8	339.3
	20	4.2	6.9	45.5	633.2
	30	4.3	6.7	49.4	809.0
ZrO_2-coated $LiCoO_2$	1	2.8	32.7	47.5	14.1
	10	1.9	45.4	42.8	21.9
	20	1.8	46.5	43.4	26.6
	30	2.8	23.7	47.1	38.9

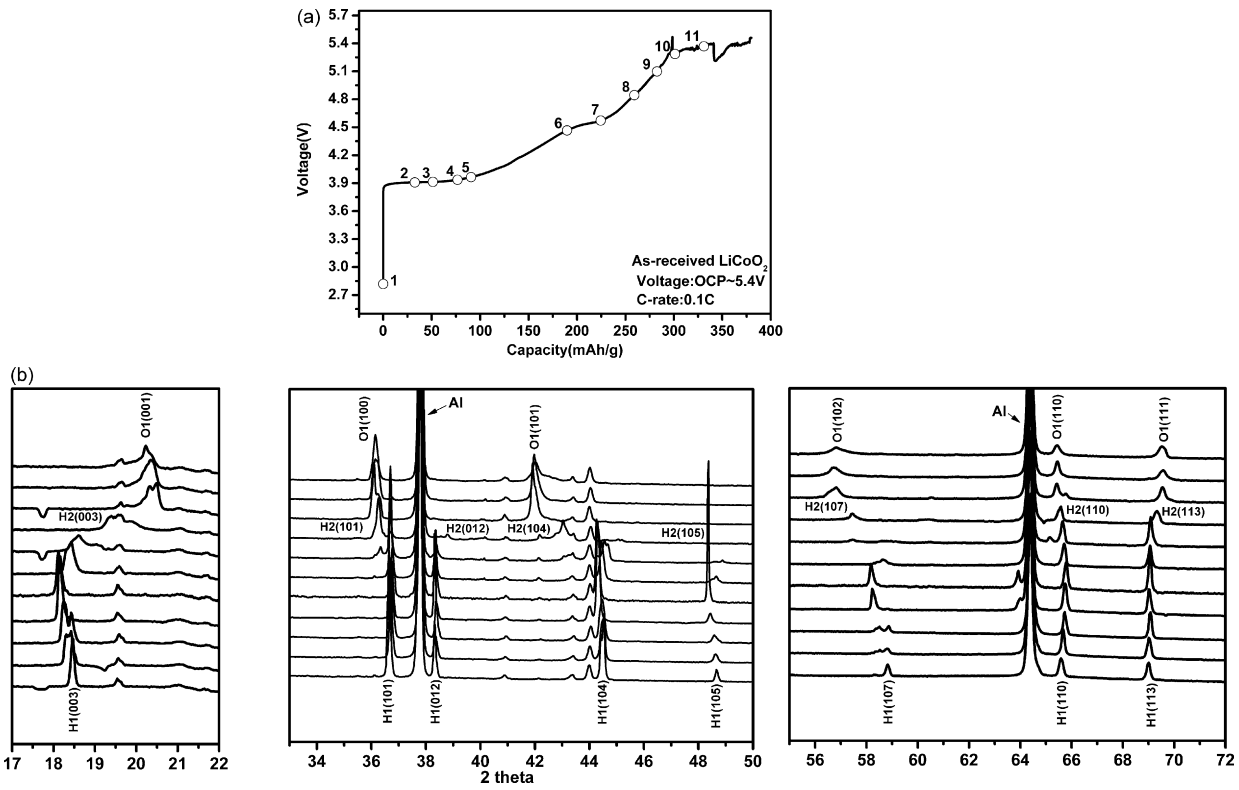

Fig. 4. (a) The 1st charge curve of the Li cell assembled with the as-received $LiCoO_2$ electrode and (b) the in situ XRD patterns collected at the corresponding charge state during 1st charge process.

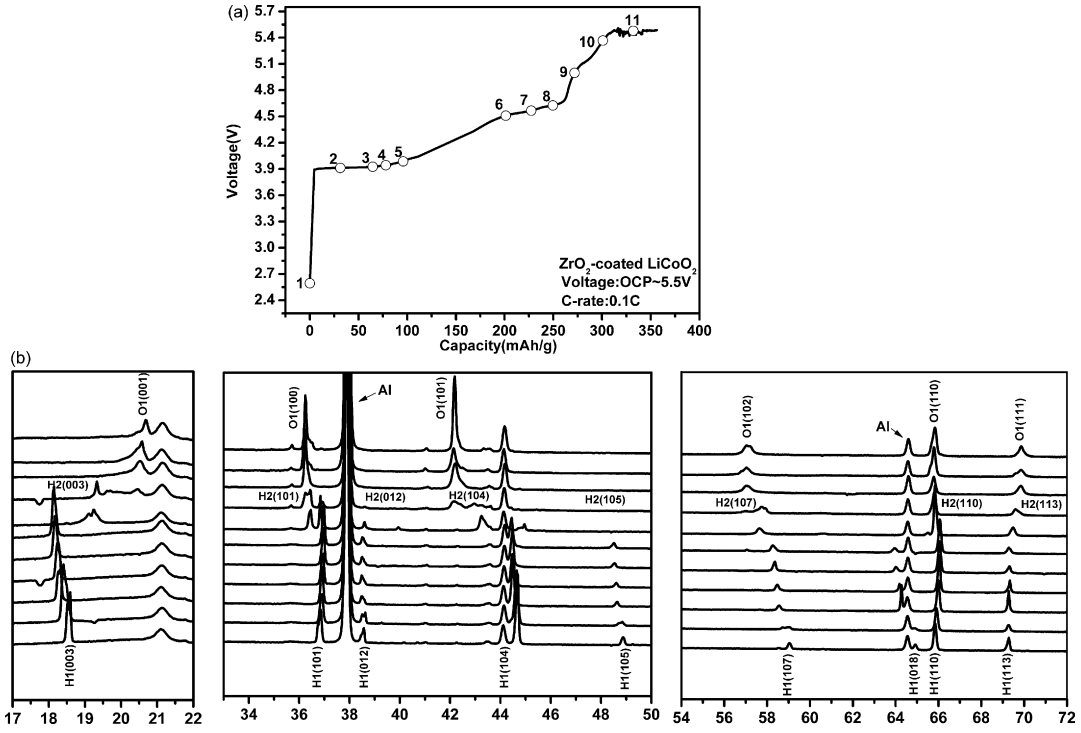

Fig. 5. (a) The 1st charge curve of the Li cell assembled by the ZrO_2-coated $LiCoO_2$ electrode and (b) the in situ XRD patterns collected at the corresponding charge state during 1st charge process.

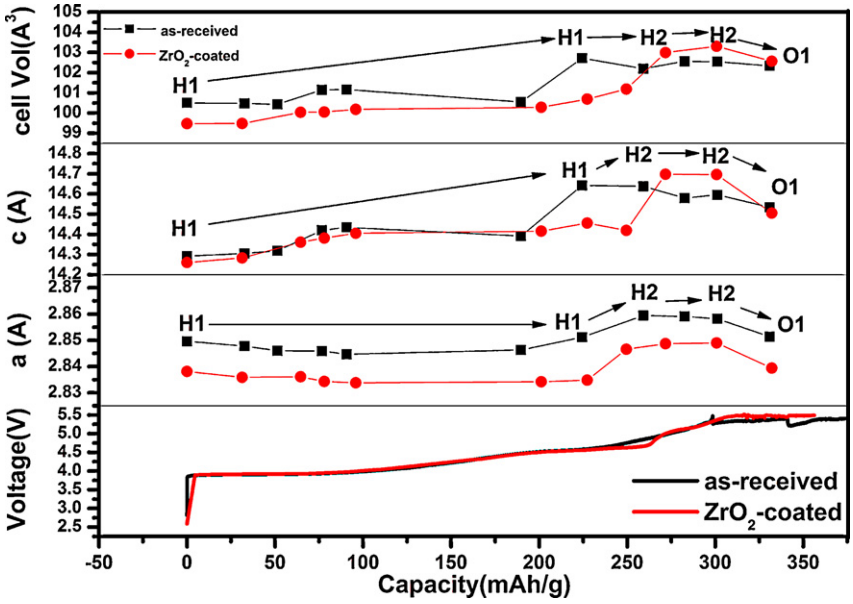

Fig. 6. Lattice parameter and phase changes of the as-received and ZrO_2-coated $LiCoO_2$ as a function of capacity during first charge in the voltage range between 2.5 and 5.4 V.

[27]. Use of this algorithm to study cobalt dissolution in $LiCoO_2$ and $LiCoO_2$ coated with ZrO_2 would be interesting and is expected to give more insights. However, this is beyond the scope of the present paper and would be dealt with elaborately elsewhere. The dissolved cobalt may cause re-deposition on the $LiCoO_2$ surface and/or re-intercalation into the structure. If the cobalt ions available in the electrolyte are inserted in to Li_xCoO_2, they could reside at the lithium layers and encourage the cation mixing. To study the degree of cation mixing, the conventional electrolyte was modified with adding 5.5 ppm of Co and 0.01 M of $NaPF_6$. The cycle charac-

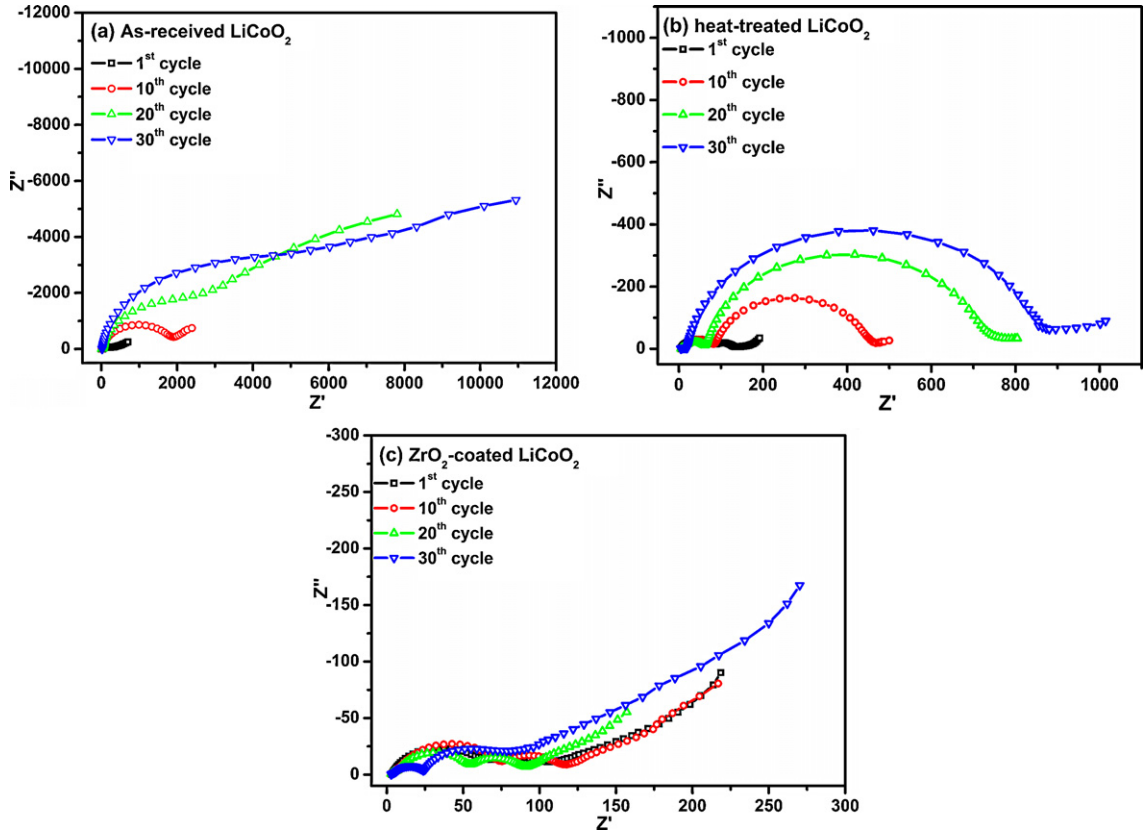

Fig. 7. EIS of the Li cells assembled with (a) as-received, (b) heat-treated, and (c) ZrO_2-coated $LiCoO_2$ respectively, as the cathode after 1st, 10th, 20th and 30th cycles in the potential range between 3.0 and 4.5 V at 0.5C.

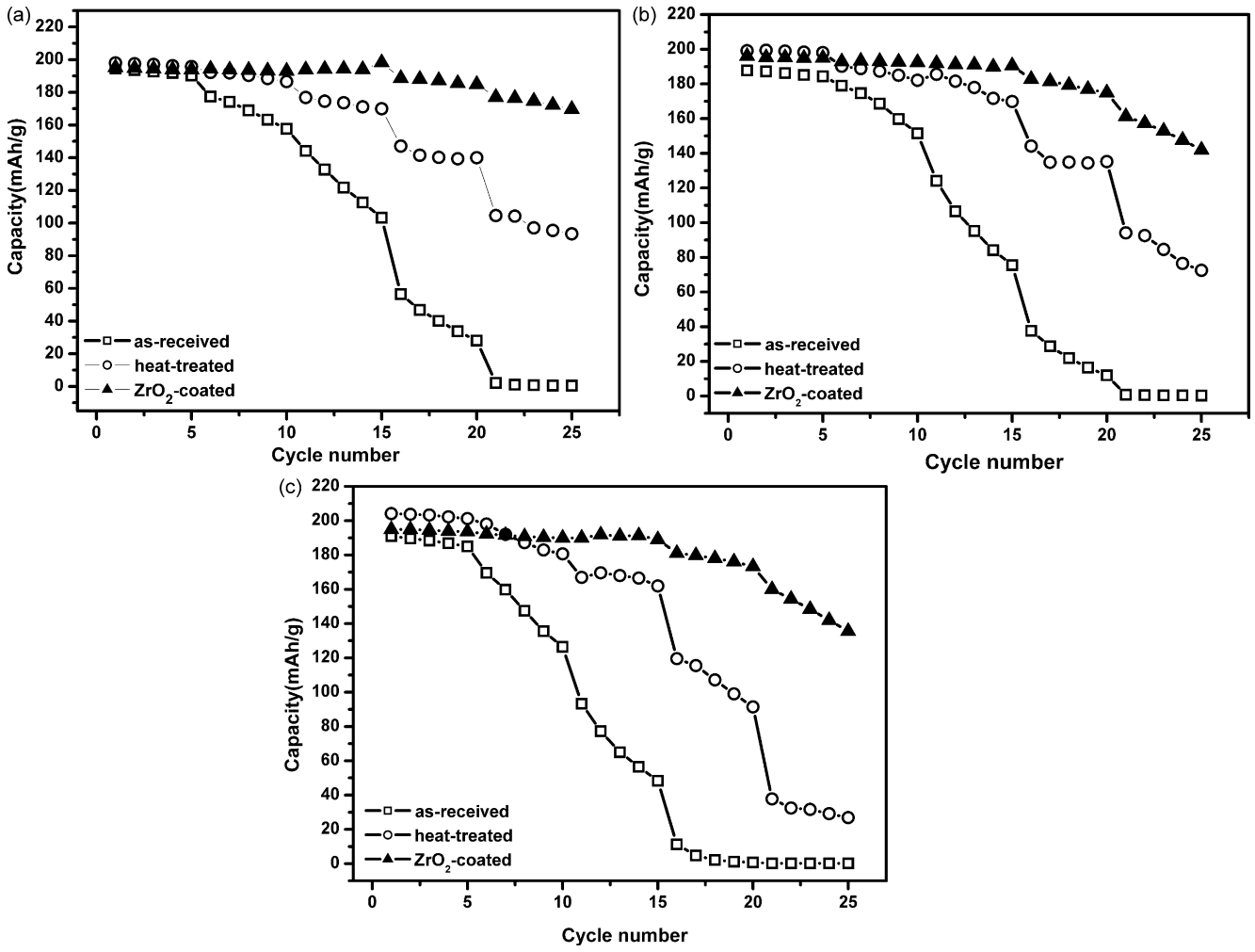

Fig. 8. Rate capability tests of the as-received, heat-treated and ZrO_2-coated $LiCoO_2$ electrodes cycling in the potential range between 3.0 and 4.5 V: 0.1*C* (1–5 cycles), 0.2*C* (6–10 cycles), 0.5*C* (11–15 cycles), 1*C* (16–20 cycles), 2*C* (21–25 cycles) and in different electrolytes: (a) 1.0 M $LiPF_6$ + EC + DEC, (b) 1.0 M $LiPF_6$ + EC + DEC + 5.5 ppm Co and (c) 1.0 M $LiPF_6$ + EC + DEC + 0.01 M $NaPF_6$.

teristics of the ZrO_2-coated, heat-treated and as-received $LiCoO_2$ electrodes charged and discharged between 3.0 and 4.5 V are compared and shown in Fig. 8. The cell was first cycled at 0.1*C* for 5 cycles followed by increasing to 2*C*. The ZrO_2-coated $LiCoO_2$ showed the highest capacity retention when cycled in all the three different electrolytes. Cation mixing was studied by calculating the *R*-factor using the following equation:

$$R\text{-factor} = \frac{Y_{\mathrm{The}} - Y_{\mathrm{Exp}}}{Y_{\mathrm{The}}}$$

where Y_{The} is the ratio of peak intensity of I_{003}/I_{104} from the XRD pattern of ideal $LiCoO_2$, and Y_{Exp} is the ratio of peak intensity of I_{003}/I_{104} from XRD pattern of $LiCoO_2$ from experiments after cycling in different electrolytes. The *R*-factor is directly proportional to cation mixing, i.e., the smaller the *R*-factor, the lower the cation mixing. The calculated results (Table 2) indicate that the *R*-factor is lower for the ZrO_2-coated $LiCoO_2$ electrode compared to that of the as-received and heat-treated electrodes in all the three electrolytes. Hence, not only the avoidance of decomposition of electrolyte, but also the higher capacity retention of ZrO_2-coated electrode could be attributed to the prevention of cation mixing during cycling when compared to the as-received and heat-treated $LiCoO_2$ electrodes.

The cutoff voltage has an influence on the electrochemical properties of the cathode material. Fig. 9 shows the charge/discharge curves of the as-received, heat-treated and ZrO_2-coated $LiCoO_2$ and the corresponding capacity retention behaviors in the voltage range of 3.0–4.2 V at a constant current density of 0.5*C*. It is obvious that all these cathodes show similar initial charge and discharge capacities ($\sim$140 mAh g^{-1}). As the cycle number increases, however, the heat-treated and ZrO_2-coated cathodes exhibit excellent capacity retention, but the as-received cathode degrades rapidly. After 30 cycles, the heat-treated and ZrO_2-coated samples maintained 94% and 97% of the initial capacities, respectively, whereas the as-received sample retained only 43% to its first-cycle capacity. The severe capacity loss of the as-received $LiCoO_2$ during cycling to 4.2 V could be the formation of surface films on the surface of the particles which isolate their electronic pathways particles from the current collector. Further the performances of the heat-treated and ZrO_2-coated samples are similar, indicating no or rare formation of the surface films on their surface. It may also tell that elimination of contaminations such as moisture and organic species on the pristine $LiCoO_2$ surface plays a key role on the inhibition of surface film formation. This result clearly demonstrates that the structural change of $LiCoO_2$ cycling up to 4.2 V is not the reason for the poor capacity retention.

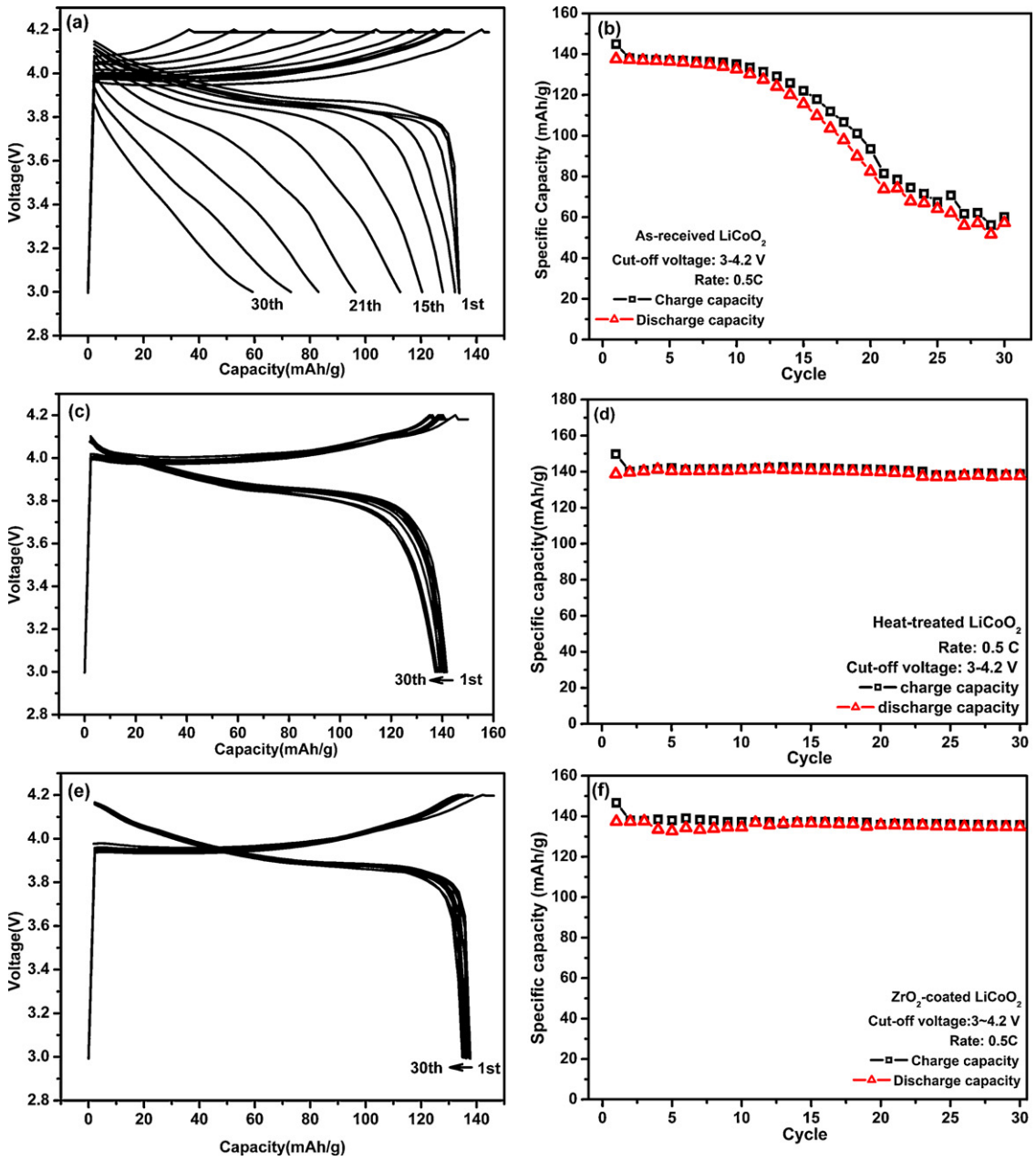

Fig. 9. Charge/discharge plots and capacity retention behaviors of the as-received (a and b), heat-treated (c and d) and ZrO_2-coated $LiCoO_2$ (e and f) electrodes cycled in the potential window of 3.0 and 4.2 V at a rate of 0.5*C*.

To understand the fading mechanism, all the three samples were cycled up to 4.5 V. The charge/discharge curves of the as-received, heat-treated and ZrO_2-coated $LiCoO_2$ and the corresponding capacity retention behaviors at a constant current density of 0.5*C* are shown in Fig. 10. It is clear that all these cathodes have similar initial charge and discharge capacities (~190 mAh g^{-1}). As the cycle number increases, the capacity fading rate is obviously different for the three different samples. After 30 cycles, the heat-treated and ZrO_2-coated samples maintain 80% and 85% of the initial capacity, respectively, whereas the as-received sample retained only 21% of its initial capacity. Undoubtedly, all the cathode materials show severe degradation for cycling up to 4.5 V. It appears that due to higher upper limit of the potential window (4.5 V), severe electrochemical decomposition at the SEI triggers the formation of a highly resistive surface film on the surface of $LiCoO_2$ causing capacity fading. Further, the cation mixing from the re-intercalation of the dissolved Co^{2+} may contribute severe fading as well. Among the heat-treated and the ZrO_2-coated sample, the latter shows a reduced cell polarization and better cycling performance. This provides further evidence that the ZrO_2-coating layer provides some protection for the surface of the $LiCoO_2$ form and reduces the electrolyte decomposition at higher voltages.

The rate capability, especially the high rate discharge performance is another important aspect for use of $LiCoO_2$ in many applications. To compare the rate capability of all the three $LiCoO_2$ samples, the charge and discharge cutoff voltages were fixed to 4.5 and 3.0 V, respectively. Rates up to 2*C* have been investigated and the results are shown in Fig. 11. It is noticed that about 85%, 48%, and 0% of the first-cycle reversible capacity can be obtained at 2*C* for the ZrO_2-coated, heat-treated and as-received $LiCoO_2$, respectively. The superior rate capability of the ZrO_2-coated $LiCoO_2$ could be attributed to less phase transformations in this potential win-

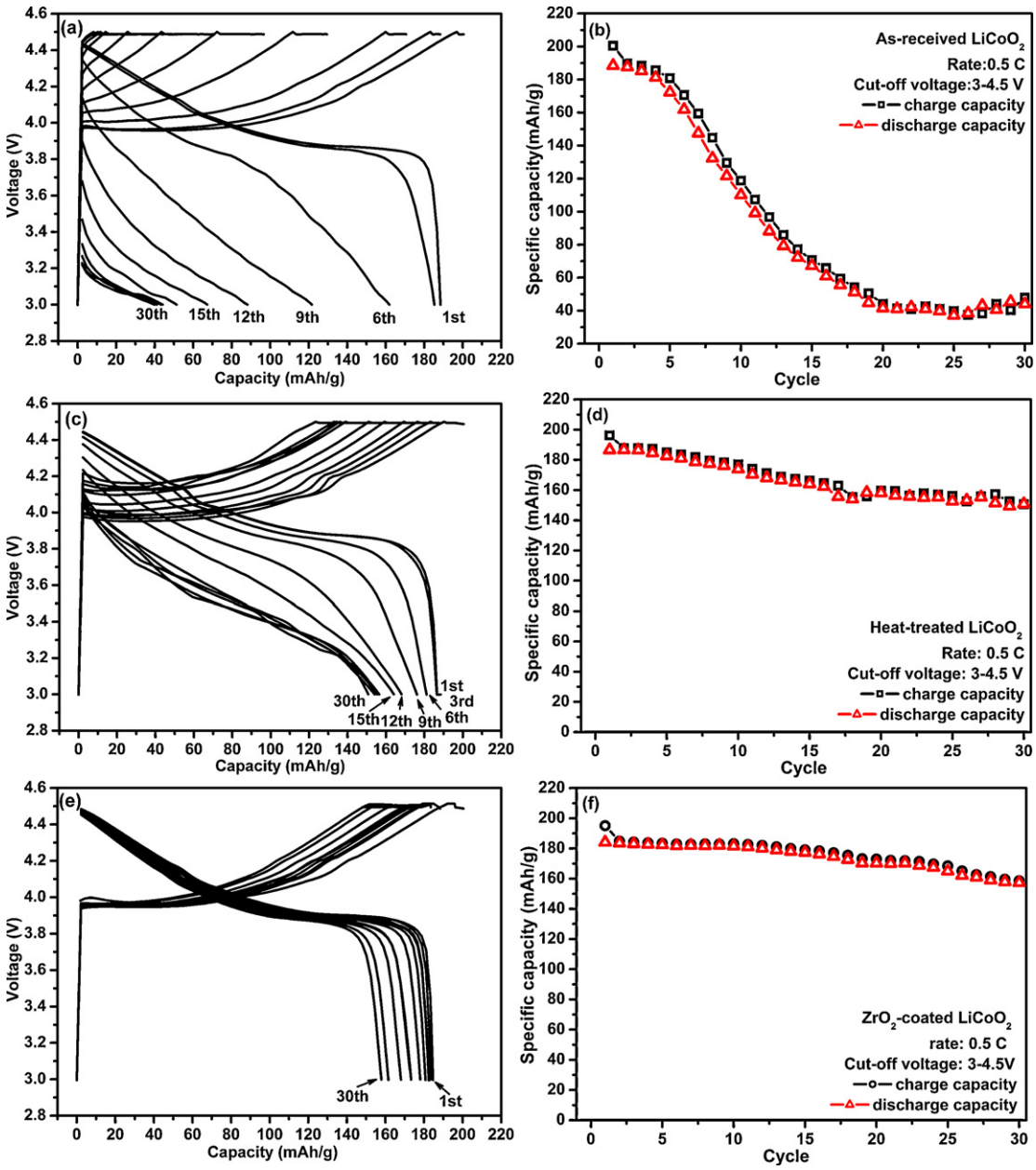

Fig. 10. Charge/discharge plots and capacity retention behaviors of the as-received (a and b), heat-treated (c and d) and ZrO_2-coated $LiCoO_2$ (e and f) electrodes cycled in the potential window of 3.0 and 4.5 V at a rate of 0.5C.

Table 2
R-factors calculated from XRD patterns of as-received, heat-treated and ZrO_2-coated $LiCoO_2$ after cycling.

Material	*R*-factor for $LiCoO_2$[a]		
	As-received	Heat-treated	ZrO_2-coated
Before cycling	0.09	0.18	0.06
Normal electrolyte[b]	0.72	0.39	0.22
Electrolyte + 5.5 ppm Co	0.62	0.64	0.38
Electrolyte + 0.01 M $NaPF_6$	0.34	0.37	0.18

[a] *R*-factor: $(Y_{The} - Y_{Exp})/Y_{The}$, where Y_{The} is the intensity ratio I_{003}/I_{104} from XRD pattern of ideal $LiCoO_2$ and Y_{Exp} is the intensity ratio I_{003}/I_{104} from XRD pattern of $LiCoO_2$ from experiments.
[b] Normal electrolyte: 1.0 M $LiPF_6$ in EC-DEC (1:1 in volume).

dow (up to 4.5 V), the suppression of electrolyte decomposition on the surface and less cation mixing resulted from re-intercalation of dissolved Co^{2+}.

The thermal stability of cathode materials, especially at delithiated state, is an important parameter to get an understanding on the structural stability and the suitability for practical applications in lithium secondary batteries. The thermal stability of the as-received, heat-treated and ZrO_2-coated $LiCoO_2$ electrodes was conducted at the state of 4.5 V to Li using differential thermal calorimetry (DSC) (Fig. 12). The amount of heat generated for the as-received, heat-treated and ZrO_2-coated $LiCoO_2$ was 142.9 J g^{-1}, 122.9 J g^{-1}, and 115.2 J g^{-1}, respectively. It can be seen that the amount of the heat released is the least one for ZrO_2-coated $LiCoO_2$. This could be attributed to the fact that the coated ZrO_2 on the surface of the $LiCoO_2$ electrode could introduce strong Zr–O bonds on the surface which in turn lowers the oxygen activity [28]. This result clearly suggests that the ZrO_2 coating on $LiCoO_2$ protects the sur-

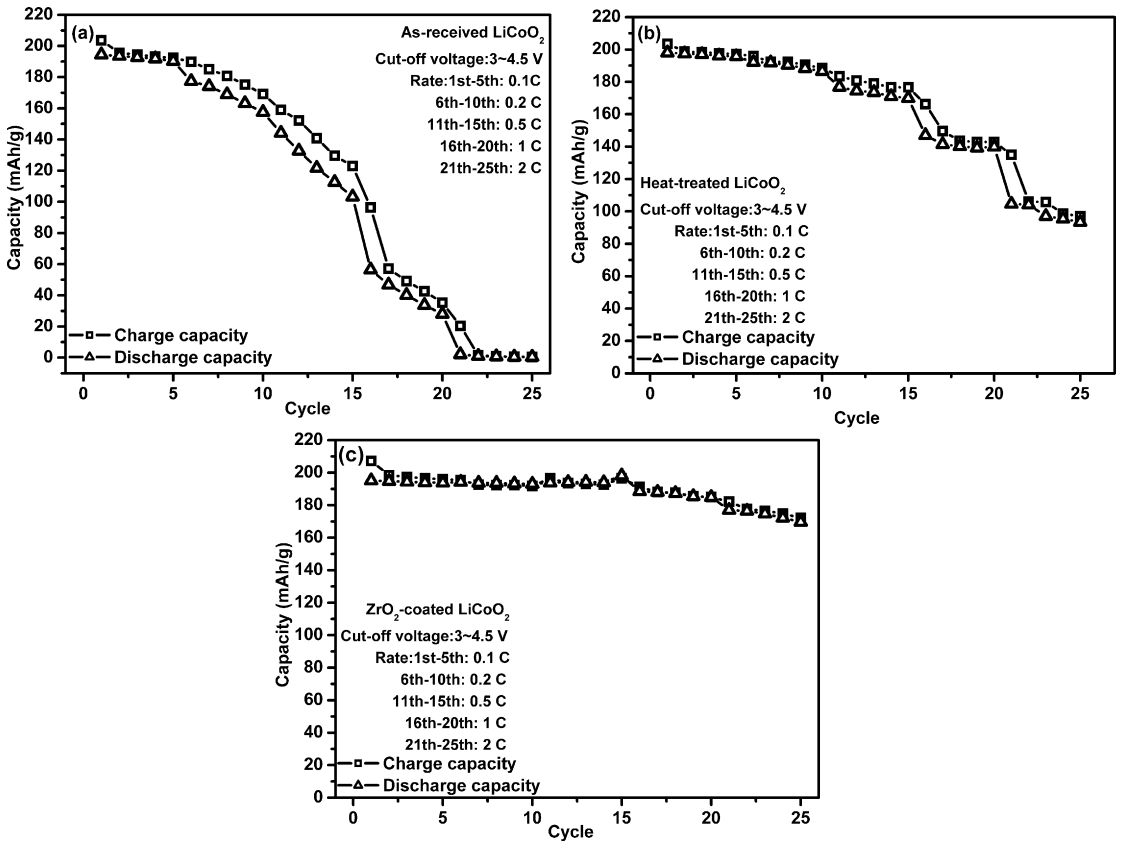

Fig. 11. Rate capability tests of the as-received (a), heat-treated (b) and ZrO_2-coated $LiCoO_2$ (c) electrodes cycled in the potential window of 3.0 and 4.2 V at a rate of 0.5C.

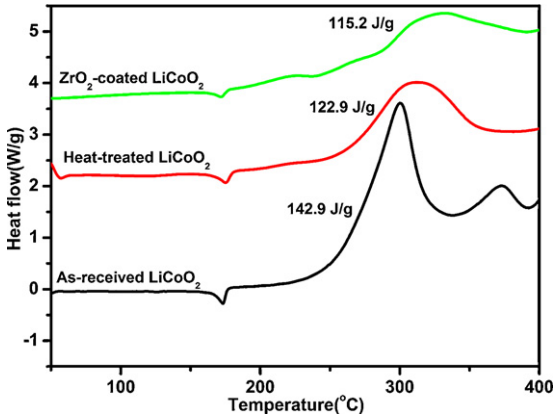

Fig. 12. DSC curves of as-received, heat-treated and ZrO_2-coated $LiCoO_2$ electrodes at the charge state of 4.5 V.

face of the active material by suppressing the generation of oxygen significantly, thereby improving the thermal stability at a higher potential range.

4. Conclusion

In this study, we have carried out a systematic investigation to understand the mechanism underlying the enhanced electrochemical performance of ZrO_2-coated $LiCoO_2$, especially in the high potential range. Superior cycling stability, rate capability and thermal stability of ZrO_2-coated $LiCoO_2$ are attributed to difference in the surface microstructure and structural stability, which subsequently leads to the less volume expansion during charging, inhibition of electrolyte decomposition and formation of surface film. Less cation mixing caused by the re-intercalation of the dissolved Co^{2+} ions by the surface ZrO_2 layer would be probably another important reason for enhanced performance.

Acknowledgements

The authors gratefully thank National Science Council (NSC, Taiwan) for the financial support (grant no. 98-ET-E-011-003-ET) and National Synchrotron Radiation Research Center (NSRRC, Taiwan) and National Taiwan University of Science and Technology (NTUST) for technical supports.

References

[1] A.R. Armstrong, P.G. Bruce, Nature 381 (1996) 499.
[2] L. Croguenner, C. Pouillerie, C. Delmas, J. Electrochem. Soc. 147 (2000) 1324.
[3] K. Mizushima, P.C. Jones, P.J. Wiseman, J.B. Goodenough, Mater. Res. Bull. 15 (1980) 1783.
[4] G. Amatucci, J.M. Tarascon, L.C. Klein, Solid State Ionics 83 (1996) 167.
[5] J. Cho, Y.J. Kim, B. Bark, Chem. Mater. 12 (2000) 3788.
[6] Z. Chen, Z. Lu, J.R. Dahn, J. Electrochem. Soc. 149 (2002) A1604.
[7] Y.J. Kim, J. Cho, T.J. Kim, B. Bark, J. Electrochem. Soc. 150 (2003) A1723.
[8] J. Cho, C. Kim, S.I. Yoo, Electrochem, Solid State Lett. 3 (2000) 362.
[9] J. Cho, Y.J. Kim, B. Park, Angew. Chem. Int. Ed. 40 (2001) 3367.
[10] Z. Chen, J.R. Dahn, Electrochem. Solid-State Lett. 5 (2002) A213.
[11] Y. Takahashi, S. Tode, A. Kinoshita, H. Fujimoto, I. Nakane, S. Fujitani, J. Electrochem. Soc. 155 (2008) A537.
[12] J. Cho, Y.J. Kim, B. Park, Chem. Mater. 12 (2000) 3788.
[13] Y.J. Kim, H. Kim, B. Kim, D. Ahn, J.G. Lee, T.J. Kim, D. Son, J. Cho, Y.W. Kim, B. Park, Chem. Mater. 15 (2003) 1505.
[14] A.M. Kannan, L. Rabenberg, A. Manthiram, Electrochem. Solid-State Lett. 6 (2003) A16.
[15] J. Cho, B. Kim, J.G. Lee, Y.W. Kim, B. Park, J. Electrochem. Soc. 152 (2005) A32.
[16] G.T.K. Fey, Z.X. Weng, J.G. Chen, C.Z. Lu, T.P. Kumar, S.P. Naik, A.S.T. Chiang, D.C. Lee, J.R. Lin, J. Appl. Electrochem. 34 (2004) 715.
[17] Z.H. Chen, J.R. Dahn, Electrochem, Solid State Lett. 7 (2004) A11.
[18] A.T. Appapillai, A.N. Mansour, J. Cho, Y.S. Horn, Chem. Mater. 19 (2007) 5748.
[19] L. Liu, L. Chen, X. Huang, X.Q. Yang, W.S. Yoon, H.S. Lee, J. McBreen, J. Electrochem. Soc. 151 (2004) A1344.

[20] Y.J. Kim, J. Cho, T.J. Kim, B. Park, J. Electrochem. Soc. 150 (2003) A1723.
[21] B.J. Hwang, R. Santhanam, C.P. Huang, Y.W. Tsai, J.F. Lee, J. Electrochem. Soc. 149 (2002) A694.
[22] S.K. Hu, G.H. Cheng, M.Y. Cheng, B.J. Hwang, R. Santhanam, J. Power Sources 188 (2009) 564.
[23] B.J. Hwang, S.K. Hu, C.H. Chen, C.Y. Chen, H.S. Sheu, J. Power Sources 174 (2007) 761.
[24] K.Y. Chung, W.S. Yoon, J. McBreen, X.Q. Yang, S.H. Oh, H.C. Shin, W.I. Cho, B.Y. Cho, J. Electrochem. Soc. 153 (2006) A2152.
[25] K.Y. Chung, W.S. Yoon, H.S. Lee, J. McBreen, X.Q. Yang, S.H. Oh, W.H. Ryu, J.L. Lee, W.I. Cho, B.Y. Cho, J. Power Sources 163 (2006) 185.
[26] D. Sherwood, B. Emmanuel, J. Cryst. Growth Des. 6 (2006) 1415.
[27] K. Ragavendran, D. Sherwood, D. Vasudevan, B. Emmanuel, Physica B 404 (2009) 2166.
[28] M.M. Thackeray, C.S. Johnson, J.S. Kim, K.C. Lauzze, J.T. Vaughey, N. Dietz, D. Abraham, S.A. Hackney, W. Zeltner, M.A. Anderson, Electrochem. Commun. 5 (2003) 752.